

Thermal Dissociation of Gaseous Bradykinin Ions

David J. Butcher,[†] Keiji G. Asano,[‡] Douglas E. Goeringer,[‡] and Scott A. McLuckey^{*,‡}

Chemical and Analytical Sciences Division, Oak Ridge National Laboratory, Oak Ridge, Tennessee 37831-6365, and Department of Chemistry and Physics, Western Carolina University, Cullowhee, NC 28723

Received: July 20, 1999; In Final Form: September 15, 1999

Singly, doubly, and triply charged bradykinin ions have been dissociated thermally in a quadrupole ion trap operated with a bath gas comprised principally of helium at 1 mTorr. Dissociation rates as a function of bath gas temperature were measured along with product ion spectra. Studies were conducted to show that dissociation rates were independent of ion storage conditions and bath gas pressure. These studies indicate that good approximations to true Arrhenius parameters could be determined from Arrhenius plots using the bath gas temperature as a measure of the internal energy distribution of the parent ion population. Arrhenius parameters derived in this work agree with those reported recently using blackbody-induced radiative dissociation for the singly and doubly charged ions within experimental error. The spectrum of dissociation products were also very similar, reflecting the equivalency of the two methods for deriving Arrhenius parameters. Arrhenius parameters for the triply charged ion ($E_a = 0.79 \pm 0.03$ eV; $\log A = 9.3 \pm 0.36$ s⁻¹) are reported for the first time. Comparison of the Arrhenius parameters for the doubly and triply charged parent ions, along with dissociation reactions of the ions formed via water loss from the two parent ions indicate that water loss reactions from doubly protonated bradykinin and from triply protonated bradykinin proceed via distinctly different mechanisms.

Introduction

Gaseous ions derived from biomolecules are playing an increasingly important role in biological research. A particularly important process is the unimolecular dissociation of gaseous bioions, which can yield important structural information. In the case of peptides, proteins, and oligonucleotides, the desired information is usually the order or sequence of the individual amino acid or nucleotide residues. A variety of factors, aside from the primary structure of the biopolymer, underlie the appearance of the spectrum of products derived from dissociation of a bioion. These include the instrumental factors associated with analysis and detection of product ions, time frame for dissociation, the method by which energy is added to the ion to induce dissociation, and the ion charge state.^{1–7} The latter factor can also interplay with three-dimensional structural effects that apparently can perform major roles in determining favored dissociation pathways.^{8–11}

A wide variety of means have been used to activate bioions, including both single and multiple collisions at kiloelectronvolt¹² and electronvolt¹³ collision energies (laboratory reference frame), collisions with surfaces,¹⁴ single UV photon photodissociation,¹⁵ and infrared multiphoton dissociation,¹⁶ among others. In some cases, the energy to drive dissociation is deposited in the course of the ion formation process, as with so-called postsource decay¹⁷ associated with matrix-assisted laser desorption ionization. Also, energy liberated in the course of exoergic electron capture¹⁸ or electron transfer¹⁹ processes involving multiply charged bioions can drive fragmentation. These activation processes represent a remarkably wide range of activation times

and energy transfer distributions. While all enjoy some degree of success in yielding structural information via the identities of the product ions, absolute information regarding the energetic and entropic requirements of the various competing dissociation reactions is usually difficult to derive because the internal energy distributions of the activated ions are not well characterized. A particularly important special case, however, is when the parent ion internal energy distribution is very nearly Boltzmann and can be characterized by a temperature. Such a condition can be achieved using activation methods in which ion activation, deactivation, and dissociation processes all occur in parallel.²⁰ The parent ion internal energies assume a nearly Boltzmann internal energy distribution when the rates for ion activation and deactivation are large relative to unimolecular dissociation rates. This condition has been referred to as rapid energy exchange.²¹ Under this condition, reasonably accurate Arrhenius parameters can be obtained by measuring dissociation rates as a function of parent ion temperature. Under conditions in which activation rates are either lower than or comparable to unimolecular dissociation rates, experimentally observed dissociation rates are determined either by the activation rate or a combination of activation rate and unimolecular dissociation rates.^{22,23}

It has recently been shown that ions stored in a low-pressure environment can undergo unimolecular dissociation during the course of emission and absorption of radiation to and from the walls of the storage device.^{24,25} For relatively small ions, the dissociation rate is largely determined by the absorption rate,^{22,23} whereas for ions with many degrees of freedom, such as bioions, the rate-determining step can be the unimolecular dissociation rate. The latter condition has been exploited to measure Arrhenius activation parameters associated with dissociation of ions derived from biopolymers.^{10,21,26} The technique has been denoted blackbody-induced radiative dissociation (BIRD). An

* Corresponding author. Phone: (423)574-2848. Fax: (423)576-8559. E-mail: mcluckeysa@ornl.gov.

[†] Western Carolina University.

[‡] Oak Ridge National Laboratory.

obvious alternative to BIRD, which relies on radiative transitions for ion activation and deactivation, is thermal dissociation that relies on collisions for mediating energy transfer. In fact, collisional thermal dissociation has been effected in electrospray ionization ion sources.^{27–30} However, the latter studies did not enjoy the benefits of tandem mass spectrometry whereby parent ion/product ion relationships can be determined with confidence.

We have recently demonstrated thermal dissociation of protonated leucine enkephalin in a quadrupole ion trap mass spectrometer using a bath gas (principally helium) at 1 mTorr.³¹ Herein, we relate the thermal dissociation behavior of singly, doubly, and triply protonated bradykinin. These results augment those describing the dissociation of bradykinin ions collisionally activated under other conditions.^{32–36} BIRD results have already been presented for the singly and doubly protonated species,^{10,26} which therefore provides a basis for comparison for techniques that should yield equivalent information. Data for the triply protonated ion have not yet been presented in the literature. We show here that the thermal dissociation data for the singly and doubly charged ions are very similar to the results reported by BIRD both in terms of the activation parameters derived from dissociation kinetics and in the appearance of the product ion spectra. These results suggest that the internal temperatures of the bradykinin parent ions can be taken as the bath gas temperature, at least over the dissociation rate range accessed in this work. The quadrupole ion trap, therefore, with its capabilities for multiple stages of mass spectrometry, is a flexible tool for deriving Arrhenius parameters for gaseous bioions via thermal dissociation.

Experimental Section

Bradykinin (Arg-Pro-Pro-Gly-Phe-Ser-Pro-Phe-Arg or RP-PGFSPFR) obtained commercially (Sigma, St. Louis, MO) was dissolved in a solution of 50:50 methanol/water to a concentration of roughly 1000 μM with 1% acetic acid. Working solutions for normal electrospray ($\sim 20 \mu\text{M}$) were prepared by diluting the stock solution with 99% methanol/1% acetic acid. The solution was infused at a rate of 1.0 $\mu\text{L}/\text{min}$ through a 100 μm i.d. stainless steel capillary held at +3.5–4.0 kV for production of the $(\text{M}+\text{H})^+$ and $(\text{M}+2\text{H})^{2+}$. A nanospray needle was used to produce the $(\text{M}+3\text{H})^{3+}$ ions. In this case, a 99% water/1% acetic acid solution was used to dilute the 1000 μM stock solution.

All experiments were performed with a Finnigan ion trap mass spectrometer (ITMS, San Jose, CA), modified for electrospray ionization. An electrospray interface/ion injection lens/ion trap assembly, which has been described previously,³⁷ was attached to the vacuum system of the ITMS. The ITMS vacuum system is equipped with infrared heaters and a closed-loop temperature control system. It was found that the bath gas could best be maintained at a constant temperature by suspending the platinum resistance thermometer of the temperature control system in the vacuum system (i.e., it was disconnected from its normal attachment to the surface of the vacuum system). The location of the platinum resistance thermometer is somewhat remote from the ion trap itself. The temperature indicated by the platinum resistance thermometer was therefore calibrated against a temperature measurement made by suspending a temperature probe (Omega) adjacent to the ion trap (in the absence of any applied voltage) and systematically altering the temperature set point of the temperature feedback system. Essentially identical temperatures were also measured when the probe was physically touching a mounting bracket of the ion trap electrodes. Unless otherwise indicated, helium was intro-

duced into the vacuum chamber to a total pressure of 1 mTorr, as measured on an ion gauge and corrected for response to helium.

Following an ion accumulation period of 100–300 ms, bradykinin ions were isolated using a single resonance ejection ramp. That is, isolation of the parent ion of interest was effected using a single scan of the rf-voltage amplitude applied to the ring electrode while simultaneously applying a single frequency in dipolar fashion chosen to sweep out ions of m/z greater than that of the ion of interest. Lower m/z ions were swept out by passing the ions through the $q_z = 0.908$ exclusion limit. A relatively broad ion isolation window (i.e., several m/z units) was employed to avoid collisional activation of the parent ion by off-resonance power absorption due to the isolation step.

The rates of dissociation of the parent ions were measured by recording the product ion mass spectra as a function of reaction time and as a function of bath gas temperature. At each temperature, product ion spectra were obtained over reaction periods extending to as long as 50 s. The spectrum used for each reaction time was the average of 25–200 repetitions of the experimental sequence described above. Dissociation rate data were derived from plots of $\ln[P]/([P + \Sigma F]_t)$ versus time, where P is the parent ion abundance and ΣF represents the sum of the intensities of all product ions. The use of $[P + \Sigma F]$ in the denominator is intended to normalize for nondissociative parent ion loss. However, over the time ranges used in this work, total ion losses were typically less than 10%.

Results and Discussion

Dissociation Kinetics. Two important considerations must be addressed in interpreting dissociation rates derived from ion activation in a quadrupole ion trap. The first is establishing whether the parent ion population undergoing fragmentation approaches the rapid energy exchange condition. If so, the ions can be characterized with a temperature and activation parameters can be determined with deviations from true Arrhenius parameters within the experimental error of the dissociation rate measurements. The second is determining the temperature that characterizes the parent ion population. Each issue is discussed in turn below beginning with the subject of ion internal temperature.

In the absence of external electric fields, the temperature of the bath gas characterizes an ion population undergoing thermal dissociation in the rapid energy exchange limit. In the case of the ion trap, however, there is the possibility that ions can absorb power from the radio frequency electric field that gives rise to the trapping potential resulting in inelastic collisions with the bath gas and an elevation of ion internal temperature relative to the bath gas temperature. Such an rf-internal heating effect arises from the micromotion imposed upon an ion stored in a quadrupole ion trap.³⁸ This effect is exploited in the so-called “boundary activation” technique,^{39–49} whereby potentials are applied to the ion trap electrodes to bring parent ions in close proximity to a so-called “stability boundary”. Under this condition, ions absorb power from the drive rf and can be activated by inelastic collisions.

We have recently studied the rf-internal heating phenomenon with protonated leucine enkephalin serving as a thermometer ion⁵⁰ and found that no measurable change in the dissociation rate of protonated leucine enkephalin was observed until ions were situated very near to a stability boundary. However, effective parent ion temperatures of as high as 170 K over the bath gas temperature could be readily achieved by bringing ions close to a stability boundary. Furthermore, in a recent study of

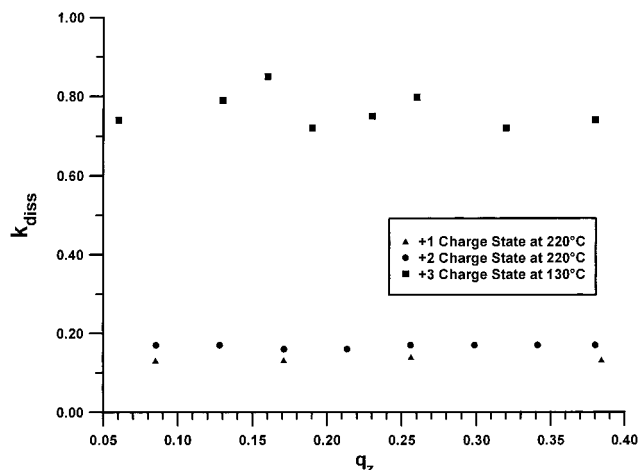


Figure 1. Experimentally observed dissociation rate, k_{diss} , versus q_z for the bradykinin (M+H)⁺ ion at 220 °C (triangles), the bradykinin (M+2H)²⁺ ion at 220 °C (filled circles), and for the bradykinin (M+3H)³⁺ ion at 130 °C (filled squares).

the thermal dissociation of protonated leucine enkephalin, no effect on the dissociation rate was observed when parent ions were stored with $a_z = 0$, $q_z = 0.075$ – 0.3 .³¹ The dimensionless parameters q_z and a_z are commonly used to indicate the conditions of storage for an ion in a quadrupole ion trap and, for ion trap electrodes of hyperbolic shape,⁵¹ are defined as

$$q_z = -2q_r = -8eV/[m\Omega^2(r_0^2 + 2z_0^2)] \quad (1)$$

and

$$a_z = 2a_r = -16eU/[m\Omega^2(r_0^2 + 2z_0^2)] \quad (2)$$

where V is the amplitude of the radio frequency voltage (applied to the ring electrode in this work), m is the mass of the ion, Ω is the drive rf frequency, r_0 is the inner radius of the ring electrode, $2z_0$ is the minimum distance between the end-caps, and U is the dc voltage applied to the ring-electrode (which was 0 V throughout this study, i.e., $a_z = 0$). The range of q_z of 0.075–0.3 ($a_z = 0$) is relatively remote from an ion storage boundary. Figure 1 shows experimentally observed values of dissociation rate, k_{diss} , as a function of q_z over the range of 0.05–0.4 for the bradykinin (M+H)⁺ ion at 220 °C (k_{diss} of roughly 0.17 s⁻¹), the bradykinin (M+2H)²⁺ ion at 220 °C (k_{diss} of roughly 0.18 s⁻¹), and for the bradykinin (M+3H)³⁺ ion at 130 °C (k_{diss} of roughly 0.76 s⁻¹). These results, like those observed for protonated leucine enkephalin, indicate that rf-internal heating is too small to affect the dissociation rates for these ions to a measurable extent. The bath gas temperature is therefore a good approximation for the parent ion internal energy distribution, provided the ions approach the rapid energy exchange limit.

For the (M+H)⁺ and (M+2H)²⁺ ions, where direct comparisons can be made with the BIRD studies,^{10,26} the dissociation rates measured here fall within the range of those reported using BIRD. Assuming the BIRD measurements were acquired under rapid energy exchange conditions, and evidence was presented that they were, it stands to reason that the ion trap measurements were also acquired under rapid energy exchange conditions when it is considered that the ion trap measurements were made at pressures roughly 5 orders of magnitude greater than those applicable to the BIRD studies. (The ion/helium collision rate in the ion trap is roughly 10⁵ s⁻¹, assuming a 250 Å² collision cross section for the bradykinin ions.^{52,53}) Under rapid energy

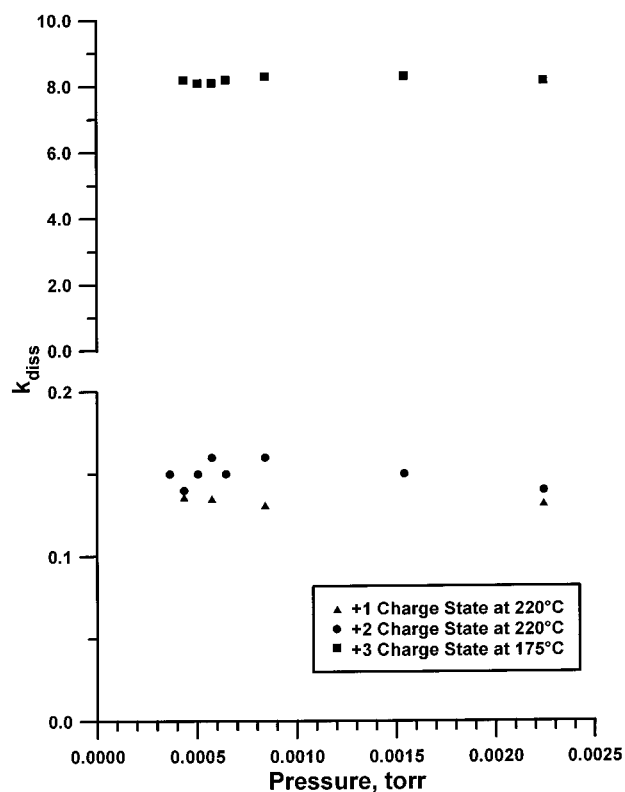


Figure 2. Experimentally observed dissociation rate, k_{diss} , versus bath gas pressure plots for the (M+H)⁺ ion at $T = 220$ °C (triangles), the (M+2H)²⁺ ion at $T = 220$ °C (filled circles), and the (M+3H)³⁺ ion at $T = 175$ °C (filled squares).

exchange conditions, the measured k_{diss} values should be independent of pressure. Figure 2 shows k_{diss} versus bath gas pressure plots for the (M+H)⁺ ion at $T = 220$ °C, the (M+2H)²⁺ ion at $T = 220$ °C, and the (M+3H)³⁺ ion at $T = 175$ °C. Clearly, there is no measurable pressure effect on k_{diss} over the limited pressure range of Figure 2. A wider range of pressure is precluded on the low side by increasingly inefficient trapping of ions injected from the external ion source as the bath gas pressure decreases. On the high-pressure side, detector noise becomes a limitation. Of the three parent ions subjected to study here, the (M+3H)³⁺ ion might be expected to be most likely to show pressure-dependent rate behavior because the dissociation rates measured for this ion tended to be significantly higher than those of the singly and doubly protonated species at the same temperatures. However, no pressure effect was noted for the (M+3H)³⁺ ion, and each parent ion showed linear $\ln k_{\text{diss}}$ vs $(kT)^{-1}$ plots (i.e., Arrhenius plots) over the entire k_{diss} range studied.

The $\ln[P]/([P + \Sigma F]_i)$ versus time plots for the (M+3H)³⁺ ion are shown in Figure 3. Qualitatively similar plots were also obtained for the (M+2H)²⁺ and (M+H)⁺ ions (data not shown). In all cases, the $\ln[P]/([P + \Sigma F]_i)$ versus time lines extrapolated to zero at zero time, within experimental error. A significant induction period before pseudo-first-order decay of the bradykinin (M+H)⁺ ion, on the other hand, was noted in the BIRD study.¹⁰ This delay was attributed to a slow isomerization process that preceded loss of ammonia. The absence of an induction period in this study may imply that the ions were already isomerized by the time they were isolated. It is also possible that ion activation upon ion isolation via off-resonance power absorption could drive an isomerization process. However, relatively broad ion isolation windows were used here to avoid collisional activation of the parent ions.

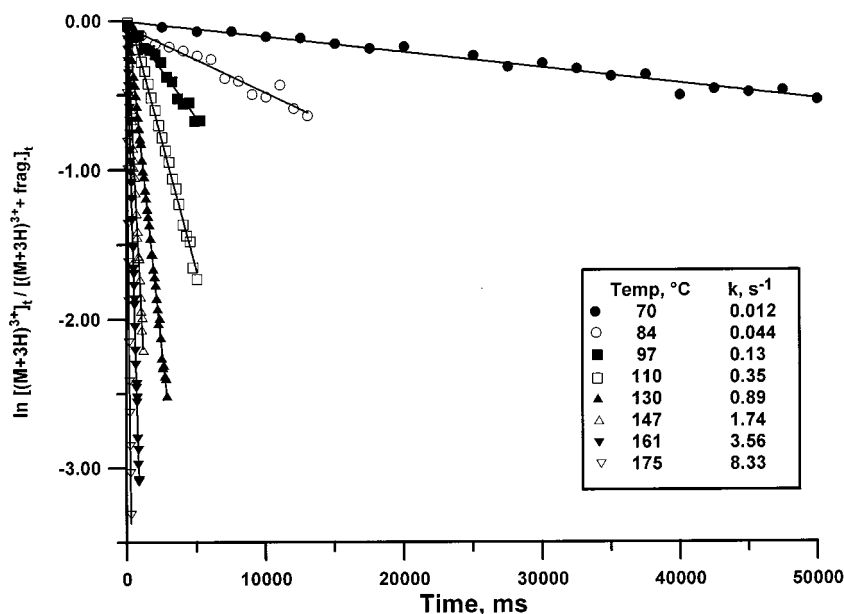


Figure 3. $\ln[P]_0/([P] + \Sigma F)_t$ versus time plots for the bradykinin $(M+3H)^{3+}$ ion at various bath gas temperatures (see insert for temperature symbols).

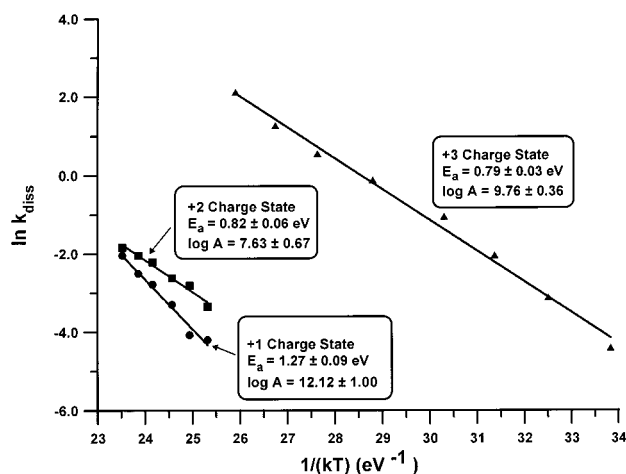


Figure 4. Arrhenius plots obtained for the $(M+H)^+$, $(M+2H)^{2+}$, and $(M+3H)^{3+}$ bradykinin ions.

TABLE 1: Arrhenius Activation Parameters Measured by Thermal Dissociation in the Quadrupole Ion Trap (This Work) and by BIRD^{10,26} and the Major Product Ion(s) Observed for Both Techniques

| BK ion | ion trap E_a (eV) | ion trap log A (s ⁻¹) | BIRD ^a E_a (eV) | BIRD log A (s ⁻¹) | major product(s) |
|---------------|---------------------------|---|------------------------------------|-------------------------------------|---------------------|
| $(M+H)^+$ | 1.27 ± 0.09 | 12.12 ± 1.0 | 1.3 | 12.59 | $(M+H-NH_3)^+$ |
| $(M+2H)^{2+}$ | 0.82 ± 0.06 | 7.63 ± 0.67 | 0.8 | 6.94 | y_7/b_2 |
| $(M+3H)^{3+}$ | 0.79 ± 0.03 | 9.3 ± 0.36 | N/A | N/A | $(M+3H-H_2O)^{3+}$ |

^a The BIRD study indicated that standard deviations for the activation energies for $(M+H)^+$ ion of bradykinin and its analogues were 0.03–0.1 eV and for the $(M+2H)^{2+}$ ion of bradykinin and its analogues were 0.04–0.1 eV.

Figure 4 shows the Arrhenius plots obtained for the $(M+H)^+$, $(M+2H)^{2+}$, and $(M+3H)^{3+}$ bradykinin ions. Table 1 lists the Arrhenius parameters derived from these plots along with those reported by BIRD for the $(M+H)^+$ and $(M+2H)^{2+}$ ions. The major products from the three ions are also listed. No distinction is made here between the ion trap and BIRD results for the major products because the major (and minor) products observed by both methods were the same, at least where direct compari-

sons could be made (vide infra). All three parent ions yielded linear Arrhenius plots over the rate ranges studied. Significant deviations from rapid energy exchange behavior would be expected to first appear at the highest dissociation rates, as reflected by rate data that fall below the line. Such an observation would suggest that the ions were beginning to fall into the so-called roll-over region where the activation rate begins to play an important role in determining k_{diss} . The $(M+3H)^{3+}$ ion provides the most stringent test because k_{diss} values as high as about 8 s^{-1} were used to construct the Arrhenius plot for this ion. The linearity of the Arrhenius plot at high values of k_{diss} is consistent with the pressure data of Figure 2, which suggested that even at k_{diss} values of about 8 s^{-1} the bradykinin system approaches the rapid energy exchange limit.

It is noteworthy that the Arrhenius activation parameters obtained via the thermal dissociation of bradykinin ions in the quadrupole ion trap and the BIRD results obtained using a Fourier transform ion cyclotron resonance instrument are the same within experimental error. This is the expected result provided the ions approach the rapid energy exchange limit (or, less likely, that both experiments deviate from rapid energy exchange conditions to the same extent), differences in instrumental discrimination effects in measuring parent ions and product ions are minimal, and the temperature measurements are consistent. The only other systems for which both ion trap thermal dissociation data³¹ and BIRD data⁵⁴ have been reported is that of protonated leucine enkephalin and its major product ion, b_4^+ . In the case of the $(M+H)^+$ ion, ion trap thermal results ($E_a = 1.28 \pm 0.08 \text{ eV}$; $\log A = 12.55 \pm 0.87 \text{ s}^{-1}$) and the BIRD results ($E_a = 1.09 \pm 0.06 \text{ eV}$; $\log A = 10.5 \pm 0.6 \text{ s}^{-1}$) were not the same within experimental error. However, the results obtained for the b_4^+ product ion via thermal dissociation in the ion trap ($E_a = 0.98 \pm 0.07 \text{ eV}$; $\log A = 10.6 \pm 0.8 \text{ s}^{-1}$) and via BIRD ($E_a = 1.06 \pm 0.02 \text{ eV}$; $\log A = 11.2 \pm 0.2 \text{ s}^{-1}$) agreed within experimental error. In contrast, thermal dissociation experiments conducted in an electrospray ion source at near atmospheric pressure²⁹ yielded a different set of activation parameters ($E_a = 1.66 \text{ eV}$; $\log A = 15.7 \text{ s}^{-1}$, error ranges not reported) for the $(M+H)^+$ ion of leucine enkephalin than either the ion trap or BIRD studies. While some speculation as to the

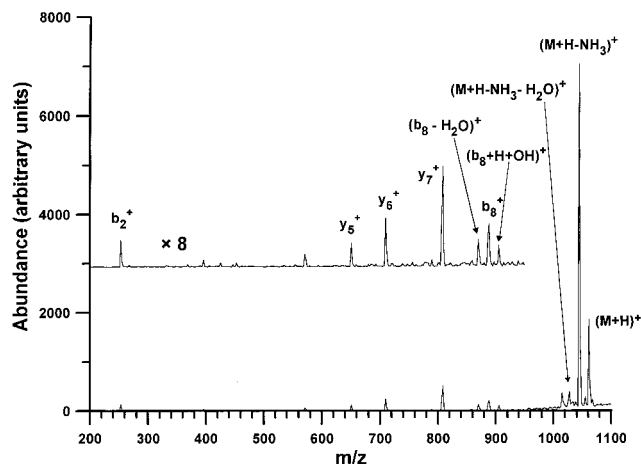


Figure 5. MS/MS spectrum of the bradykinin $(M+H)^+$ ion acquired with the ion trap after a 20 s storage period at a bath gas temperature of 213 °C.

underlying reasons for the different results obtained from these experiments might be offered, further comparisons, such as those presented here for bradykinin, are warranted before conclusions can be drawn regarding the relative merits of the various methodologies for measuring Arrhenius parameters.

Linear pseudo-first-order dissociation rate behavior was noted for all of the parent ion charge states in this work and in the reported BIRD studies. This is noteworthy in light of studies of nonfragmenting bradykinin ions that suggest that multiple noninterconverting conformations of at least some of the charge states of the ions can coexist at room temperature. For example, multiple conformations of the $(M+H)^+$ ions have been suggested by high-resolution ion mobility measurements,⁵³ although all conformations appear to fall within a narrow range of cross sections. Neither H/D exchange measurements using D_2O ^{55,56} nor hydroiodic acid attachment rate measurements⁵⁷ indicated noninterconverting mixtures of reactive conformations of the $(M+H)^+$ ion. In contrast, both the kinetics of H/D exchange with D_2O ⁵⁵ and HI attachment rate measurements⁵⁷ indicated at least two reactive conformations of the $(M+2H)^{2+}$ bradykinin ion. However, it was demonstrated in the latter study that collisional heating of the slow reacting component of the $(M+2H)^{2+}$ ion population resulted in isomerization to a mixture of fast- and slow-reacting species. The dissociation spectra of the fast- and slow-reacting species were indistinguishable. These results, and the thermal dissociation rate measurements reported here, suggest that the doubly protonated bradykinin ions probably dissociate from a common interconverting mixture of conformations. Similarly, H/D exchange measurements using deuterioiodic acid⁵⁷ indicated at least two noninterconverting reactive bradykinin $(M+3H)^{3+}$ populations at room temperature. However, the dissociation rate measurements reported here suggest that either all noninterconverting mixture components fragment with very similar Arrhenius parameters or, more likely, that the ions can freely interconvert so that they fragment from a common set of structures.

Dissociation Channels. Although the MS/MS spectra in this study and the BIRD study were acquired using significantly different approaches to mass analysis and detection, the major product ions (and essentially all of the minor product ions) reported with BIRD^{10,26} and reported here appear to be the same for the $(M+H)^+$ and $(M+2H)^{2+}$ ions. For example, Figure 5 shows the MS/MS spectrum of the bradykinin $(M+H)^+$ ion acquired with the ion trap after a 20 s storage period at a bath gas temperature of 213 °C. By far, the major product ion arises

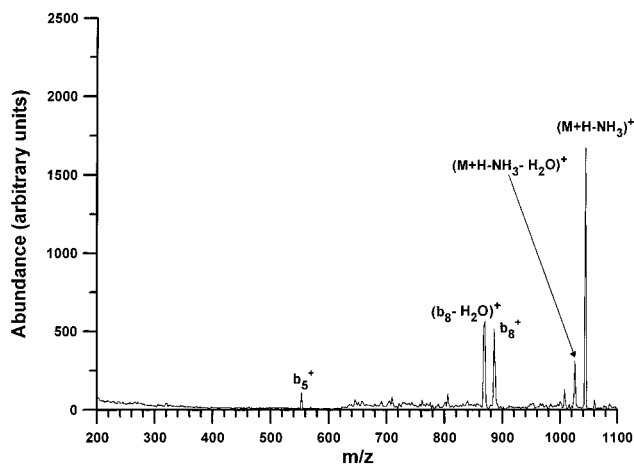


Figure 6. MS³ spectrum involving the sequence $(M+H)^+ \rightarrow (M+H-NH_3)^+ \rightarrow$ products after isolation of the $(M+H-NH_3)^+$ first generation product and storage for 30 s at a bath gas temperature of 220 °C.

from the loss of ammonia, as was also observed from BIRD, although some contribution from water loss cannot be precluded in our studies. Furthermore, as the bath gas temperature increased beyond about 200 °C, other minor fragmentation processes began to contribute to the data, just as was reported in the BIRD study. The identities and abundances of the products from these minor channels appear to be very similar to those reported using BIRD. This behavior is further evidence for the equivalency of ion trap thermal dissociation and BIRD. That is, the ions are observed to fragment at very similar rates over the same temperature range, thereby yielding similar Arrhenius activation parameters, and the identities and abundances of the various product ions are also similar.

The loss of ammonia from the $(M+H)^+$ ion has been discussed in terms of the interaction of the terminal arginines²⁶ and is consistent with a compact structure, as indicated by ion mobility measurements.⁵³ Small signals above m/z 1000 are also observed that can be attributed to the consecutive loss of ammonia and water, viz. the $(M+H-NH_3-H_2O)^+$ ion, and an ion corresponding to $(M+H-HN=C=NH)^+$. The latter ion has been implicated as an intermediate in the appearance of $(M+H-60)^+$ product ions observed in the dissociation of protonated peptides with a C-terminal arginine.³⁴ A significant signal corresponding to the $(M+H-60)^+$ ion from bradykinin was not observed in this work, although it has been observed using beam-type tandem mass spectrometry.³⁴ A small signal that can be attributed to a $(b_8+H+OH)^+$ ion ($b_8 = RPPGFSPF$) also appears in Figure 5. This ion was reported to be the most abundant product in the spectrum of metastable bradykinin $(M+H)^+$ ions formed by fast atom bombardment in a hybrid sector/quadrupole tandem mass spectrometer.⁵⁸ This ion was not mentioned explicitly in the BIRD studies, but a small peak was apparent in one of the published spectra acquired at 200 °C after a storage time of 30 s.¹⁰

A particularly attractive aspect to conducting thermal dissociation studies in an ion trapping instrument is the possibility for executing MSⁿ experiments to facilitate identification of parent ion/product ion relationships and for measuring directly Arrhenius parameters of product ions, as was done with the b_4^+ ion from protonated leucine enkephalin.^{31,54} The MS³ spectrum involving the sequence $(M+H)^+ \rightarrow (M+H-NH_3)^+ \rightarrow$ products is shown in Figure 6 after isolation of the $(M+H-NH_3)^+$ first generation product and storage for 30 s at a bath gas temperature of 220 °C. This experiment suggests that at least some of the b_8^+ and $(b_8-H_2O)^+$ product ion signal in

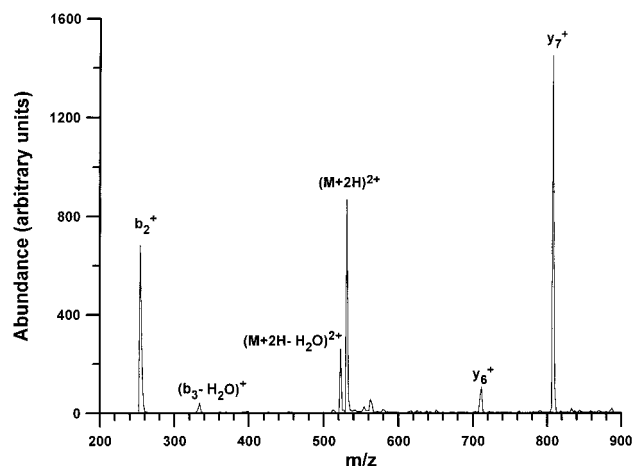


Figure 7. MS/MS spectrum of bradykinin $(M+2H)^{2+}$ via thermal dissociation after a 10 s storage period at a bath gas temperature of 213 °C.

Figure 5 can arise from sequential fragmentation from the initially formed $(M+H-NH_3)^+$ product but that the *y*-type ions (i.e., y_5^+ , y_6^+ , and y_7^+ ions, where y_5 , y_6 , and y_7 are FSPFR, GFSPFR, and PGFSPFR, respectively) are largely formed directly from the parent ion, as is the b_2^+ ion ($b_2 = RP$). Similarly, the absence of the $(b_8+H+OH)^+$ ion in Figure 6 also suggests its origin as the $(M+H)^+$ ion. The b_5^+ ion ($b_5 = RPPGF$), on the other hand, is not observed in Figure 5 and only becomes apparent at significantly longer storage times (data not shown). A lengthy induction time for the appearance of a product ion suggests that it is formed via an intermediate product ion, and Figure 6 suggests that the $(M+H-NH_3)^+$ ion is a possible precursor to the b_5^+ ion in the thermal dissociation of protonated bradykinin.

As noted in the BIRD^{10,26} and other studies, the $(M+2H)^{2+}$ ion fragments very differently than does the $(M+H)^+$ ion. Figure 7 shows the product ion spectrum derived from doubly protonated bradykinin via thermal dissociation after a 10 s storage period at a bath gas temperature of 213 °C. In this case, the formation of the y_7^+/b_2^+ complementary pair is the dominant fragmentation channel. A lesser degree of water loss is also observed. Another complementary pair, which has been attributed to $(b_3-H_2O)^+/y_6^+$ ($b_3 = RPP$), is also observed at low abundance. The $(b_3-H_2O)^+$ fragment was also observed in sustained off-resonance irradiation collisional activation studies of the $(M+2H)^{2+}$ ion wherein the mass accuracies associated with product ion mass determination were in the low ppm range.³⁵ It is curious that such an ion is formed considering that the hydroxyl groups in the molecule are on the C-terminus and the serine residue. Loss of water from the parent ion would ordinarily be expected to involve one of these hydroxyl groups. Further fragmentation of the $(M+2H-H_2O)^{2+}$ ion might then be expected to yield products that reflect water loss from either the C-terminus or the serine residue. However, if this were the case, the y_6 fragment would be expected to reflect the water loss and not the b_3 fragment. An alternative scenario is that a b_3^+/y_6^+ complementary pair is formed directly from the parent ion followed by facile loss of water from the b_3^+ product. However, no b_3^+ ion is observed even at short storage times and, in any case, it is not obvious how water loss might occur in a relatively straightforward way from the b_3^+ ion. Isolation of the y_7^+ ion and storage for tens of seconds at 220 °C yielded no measurable fragmentation precluding this ion as a possible intermediate for the formation of the lower mass product ions. An MS³ experiment, on the other hand, in which the dissociation

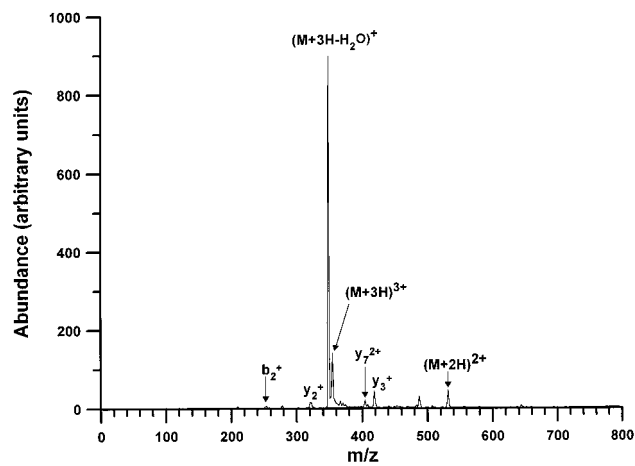


Figure 8. MS/MS spectrum of $(M+3H)^{3+}$ bradykinin ions via thermal dissociation following storage for 200 ms at a bath gas temperature of 175 °C.

products of the $(M+2H-H_2O)^{2+}$ ion were determined, showed the $(b_3-H_2O)^+/y_6^+$ complementary pair to be most abundant (data not shown). This result clearly suggests that the mechanism that gives rise to water loss from the doubly charged ion is more complex than simple loss of the serine or carboxy terminus hydroxyl group.

Triply protonated bradykinin appears to fragment almost exclusively by loss of water (a small contribution from loss of ammonia, however, cannot be precluded) as illustrated in Figure 8. This figure shows the thermal dissociation spectrum of isolated $(M+3H)^{3+}$ bradykinin ions following storage for 200 ms at a bath gas temperature of 175 °C. Clearly, this ion fragments much more rapidly at a given temperature than either the singly or doubly charged ions and follows the general trend that, as charge state increases, parent ions tend to be more readily fragmented. However, the activation energy for water loss from the $(M+3H)^{3+}$ ion is the same as the composite activation energy for fragmentation of the $(M+2H)^{2+}$ ion, within experimental error. The higher dissociation rate of the triply charged ion is a result of the roughly 2 orders of magnitude larger *A* factor. It is also interesting to note that the major fragmentation process for the $(M+3H)^{3+}$ ion does not involve charge separation, as does the major process for the $(M+2H)^{2+}$ ion. Water loss provides no obvious reduction of charge-charge repulsion in the $(M+3H)^{3+}$ ion, although a change in the location of the charges in the ion as a result of fragmentation cannot be precluded. This result therefore suggests that the addition of a third charge to bradykinin gives rise to a significant mechanistic change in the fragmentation, rather than simply lowering the activation energy for a similar process in the doubly charged ion. The dissociation behavior of the ions formed by water loss from the doubly and triply charged ions also points to a significant difference in these processes (*vide infra*).

Bradykinin also clearly illustrates the common observation that the favored dissociation channels can be highly sensitive to parent ion charge. In the case of bradykinin ions, the favored thermal dissociation processes are (i) ammonia loss for the $(M+H)^+$ ion, (ii) cleavage to yield the b_2^+/y_7^+ complementary pair for the $(M+2H)^{2+}$ ion, and (iii) water loss for the $(M+3H)^{3+}$ ion. Other product ions from thermal dissociation of the $(M+3H)^{3+}$ ion, which are given tentative assignments in Figure 8, are quite small. There is also a small signal corresponding to the $(M+2H)^{2+}$ ion that presumably arises from a low rate of proton transfer from the $(M+3H)^{3+}$ to basic neutral species present in the vacuum system at elevated temperature.

The increasing proton transfer reactivity with charge state for a given polypeptide is well-documented.^{59–63} In this case, the proton transfer rate is sufficiently small that it presents no complications in determining the dissociation rate.

Relatively little structural information is forthcoming from the thermal dissociation of the $(M+3H)^{3+}$ ion over the temperature range used to collect the data for the Arrhenius plot. At higher temperatures, dissociation rates were so high that much of the parent ion population dissociated during the ion accumulation period so as to preclude the accumulation of sufficient numbers of parent ions for precise rate measurements. However, the $(M+3H-H_2O)^{3+}$ ion could be studied at higher temperatures. For example, the $(M+3H-H_2O)^{3+}$ ion was observed to fragment almost exclusively to yield the $b_2^+/(y_7-H_2O)^{2+}$ complementary pair at a bath gas temperature of 220 °C (data not shown). This observation is consistent with the water loss coming from either the serine residue or the C-terminus (i.e., the y_7 fragment contains the serine residue and the C-terminus). This observation stands in contrast to those made for the water loss process from the $(M+2H)^{2+}$ ion. In the latter case, water loss was observed to be followed by formation of the $(b_3-H_2O)^+/y_6^+$ complementary pair. The different *A*-factors associated with water loss from the $(M+2H)^{2+}$ and $(M+3H)^{3+}$ ions and the different dissociation behaviors of the species produced by water loss, as revealed by MS^3 experiments, clearly suggests that these processes are quite different for the two charge states. Considering the low *A*-factor and curious product ions produced from the $(M+2H-H_2O)^{2+}$ ion, it appears as though water loss from the doubly charged ion proceeds via a more complex process than does water loss from the triply charged ion. The measurement of Arrhenius parameters and MS^n experiments is clearly useful in bringing this issue to light. A further delineation of the mechanisms for water loss from the various charge states of bradykinin likely requires the study of modified bradykinin ions and, perhaps, O^{18} -labeled species, which will be the subject of future work.

Conclusions

Dissociation of singly, doubly, and triply protonated bradykinin has been driven thermally in a quadrupole ion trap by heating the bath gas, which was principally comprised of helium at a pressure of 1 mTorr. Experiments conducted as a function of the storage parameter q_z over a range of 0.05–0.4 suggest that rf-heating of internal modes is sufficiently small in these studies that the parent ion internal energy distribution can be assumed to be determined by the bath gas temperature to a very good approximation. Dissociation rate data collected as a function of bath gas pressure are consistent with the ions approaching the rapid energy exchange condition, thereby making the equating of the parent ion internal temperature with the bath gas temperature a good approximation. Linear Arrhenius plots over the entire temperature range used for these ions are also consistent with close approach to the rapid energy exchange condition. Arrhenius parameters and product ion distributions for the $(M+H)^+$ and $(M+2H)^{2+}$ ions of bradykinin obtained via thermal dissociation in the quadrupole ion trap are very similar to data acquired for the same ions obtained via BIRD in a Fourier transform ion cyclotron resonance instrument. The two types of experiments are expected to be equivalent provided they both approach rapid energy exchange conditions. Arrhenius parameters for triply protonated bradykinin are reported for the first time and show the usual tendency for greater ease of fragmentation associated with more highly charged ions. However, the greater dissociation rate of the triply

charged ion appears to be due to a mechanistic effect rather than a reduction in the activation energy for dissociation. The loss of water is, by far, the dominant process for the $(M+3H)^{3+}$ ion, in contrast with loss of ammonia as the dominant process for the $(M+H)^+$ ion and formation of the b_2^+/y_7^+ complementary pair as the dominant process for the $(M+2H)^{2+}$ ion. The capability for studying thermal dissociation in an ion storage device, such as a quadrupole ion trap, is particularly attractive due to the availability of MS^n experiments for defining parent/product ion relationships. Such experiments were helpful in generating evidence that water loss from the doubly charged ion and water loss from the triply charged ion likely proceed via significantly different mechanisms.

Acknowledgment. Helpful discussions with Dr. T. Gregory Schaaff are gratefully acknowledged. Research sponsored by the Division of Chemical Sciences, Office of Basic Energy Sciences, U.S. Department of Energy, under Contract DE-AC05-96OR22464 with Oak Ridge National Laboratory, managed by Lockheed Martin Energy Research Corp. This research was supported in part by an appointment (D.J.B.) to the U.S. Department of Energy Faculty Research Participation Program at the Oak Ridge National Laboratory administered by the Oak Ridge Institute for Science and Education.

References and Notes

- (1) Smith, R. D.; Loo, J. A.; Edmonds, C. G.; Barinaga, C. J.; Udseth, H. R. *Anal. Chem.* **1990**, *62*, 882–899.
- (2) Vékey, K. *Mass Spectrom. Rev.* **1995**, *14*, 195–225.
- (3) Price, W. D.; Schnier, P. D.; Williams, E. R. *Anal. Chem.* **1996**, *68*, 859–866.
- (4) Loo, J. A.; Edmonds, C. G.; Smith, R. D. *Anal. Chem.* **1991**, *63*, 2488–2499.
- (5) Loo, J. A.; Loo, R. R. O.; Udseth, H. R.; Edmonds, C. G.; Smith, R. D. *Rapid Commun. Mass Spectrom.* **1991**, *5*, 101–105.
- (6) Loo, J. A.; Edmonds, C. G.; Smith, R. D. *Anal. Chem.* **1993**, *65*, 425–438.
- (7) McLuckey, S. A.; Habibi-Goudarzi, S. *J. Am. Chem. Soc.* **1993**, *115*, 12085–12095.
- (8) Burlet, O.; Chao-Yuh, Y.; Gaskell, S. J. *J. Am. Soc. Mass Spectrom.* **1992**, *3*, 337–344.
- (9) Wu, Q.; Van Orden, S.; Cheng, X.; Bakhtiar, R.; Smith, R. D. *Anal. Chem.* **1995**, *67*, 2498–2509.
- (10) Schnier, P. D.; Price, W. D.; Jockusch, R. A.; Williams, E. R. *J. Am. Chem. Soc.* **1996**, *118*, 7178–7189.
- (11) McLuckey, S. A.; Vaidyanathan, G. *Int. J. Mass Spectrom. Ion Processes* **1997**, *162*, 1–16.
- (12) Downard, K. M.; Biemann, K. *J. Am. Soc. Mass Spectrom.* **1994**, *5*, 966–975.
- (13) Tang, X.; Thibault, P.; Boyd, R. K. *Anal. Chem.* **1993**, *65*, 2824–2834.
- (14) Jones, J. L.; Dongré, A. R.; Somogyi, Á.; Wysocki, V. H. *J. Am. Chem. Soc.* **1994**, *116*, 8368–8369.
- (15) Williams, E. R.; Furlong, J. J. P.; McLafferty, F. W. *J. Am. Soc. Mass Spectrom.* **1990**, *1*, 288–294.
- (16) Little, D. P.; Speir, J. P.; Senko, M. W.; O'Connor, P. B.; McLafferty, F. W. *Anal. Chem.* **1994**, *66*, 2809–2815.
- (17) Spengler, B. *J. Mass Spectrom.* **1997**, *32*, 1019–1036.
- (18) Zubarev, R. A.; Kelleher, N. L.; McLafferty, F. W. *J. Am. Chem. Soc.* **1998**, *120*, 3265–3266.
- (19) Herron, W. J.; Goeringer, D. E.; McLuckey, S. A. *J. Am. Chem. Soc.* **1995**, *117*, 11555–11562.
- (20) McLuckey, S. A.; Goeringer, D. E. *J. Mass Spectrom.* **1997**, *32*, 461–474.
- (21) Price W. D.; Williams, E. R. *J. Phys. Chem. A* **1997**, *101*, 8844–8852.
- (22) Lin, C.; Dunbar, R. C. *J. Phys. Chem.* **1996**, *100*, 655–659.
- (23) Dunbar, R. C. *J. Phys. Chem.* **1994**, *98*, 8705–8712.
- (24) Thölmann, D.; Tonner, D. S.; McMahan, T. B. *J. Phys. Chem.* **1994**, *98*, 2002–2004.
- (25) Dunbar, R. C.; McMahan, T. B.; Thölmann, D.; Tonner, D. S.; Salahub, D. R.; Wei, D. *J. Am. Chem. Soc.* **1996**, *117*, 12819–12825.
- (26) Price, W. D.; Schnier, P. D.; Williams, E. R. *Anal. Chem.* **1996**, *68*, 859–866.

- (27) Rockwood, A. L.; Busman, M.; Udseth, H. R.; Smith, R. D. *Rapid Commun. Mass Spectrom.* **1991**, *5*, 582–585.
- (28) Busman, M.; Rockwood, A. L.; Smith, R. D. *J. Phys. Chem.* **1992**, *96*, 2397–2400.
- (29) Meot-ner, M.; Dongré, A. R.; Somogyi, Á.; Wysocki, V. H. *Rapid Commun. Mass Spectrom.* **1995**, *9*, 829–836.
- (30) Penn, S. G.; He, F.; Green, M. K.; Lebrilla, C. B. *J. Am. Soc. Mass Spectrom.* **1997**, *8*, 244–252.
- (31) Asano, K. G.; Goeringer, D. E.; McLuckey, S. A. *Int. J. Mass Spectrom.* **1999**, *185/186/187*, 207–219.
- (32) Kaltashov, I. A.; Fabris, D.; Fenselau, C. C. *J. Phys. Chem.* **1995**, *99*, 10046–10051.
- (33) Szilágyi, Z.; Drahos, L.; Vékey, K. *J. Mass Spectrom.* **1997**, *32*, 689–696.
- (34) Deery, M. J.; Summerfield, S. G.; Buzy, A.; Jennings, K. R. *J. Am. Soc. Mass Spectrom.* **1997**, *8*, 253–261.
- (35) Heck, A. J. R.; Derrick, P. J. *Anal. Chem.* **1997**, *69*, 3603–3607.
- (36) Schnier, P. D.; Jurchen, J. C.; Williams, E. R. *J. Phys. Chem. B* **1999**, *103*, 737–745.
- (37) Van Berkel, G. J.; Glish, G. L.; McLuckey, S. A. *Anal. Chem.* **1990**, *62*, 1284–1295.
- (38) Blatt, R.; Zoller, P.; Holzmüller, G.; Siemers, I. *Z. Phys. D* **1986**, *4*, 121–126.
- (39) Paradisi, C.; Todd, J. F. J.; Traldi, P.; Vettori, U. *Org. Mass Spectrom.* **1992**, *27*, 251–254.
- (40) Paradisi, C.; Todd, J. F. J.; Vettori, U. *Org. Mass Spectrom.* **1992**, *27*, 1210–1215.
- (41) Curcuruto, O.; Fontana, S.; Traldi, P.; Celon, E. *Rapid Commun. Mass Spectrom.* **1992**, *6*, 322–323.
- (42) Creaser, C. S.; O'Neill, K. E. *Org. Mass Spectrom.* **1993**, *28*, 564–569.
- (43) March, R. E.; Weir, M. S.; Tkaczyk, M.; Londry, F. A.; Alfred, R. L.; Franklin, A. M.; Todd, J. F. J. *Org. Mass Spectrom.* **1993**, *28*, 499–509.
- (44) Paradisi, C.; Traldi, P.; Vettori, U. *Rapid Commun. Mass Spectrom.* **1993**, *7*, 690–692.
- (45) March, R. E.; Londry, F. A.; Fontana, S.; Catinella, S.; Traldi, P. *Rapid Commun. Mass Spectrom.* **1993**, *7*, 929–934.
- (46) March, R. E.; Weir, M. R.; Londry, F. A.; Catinella, S.; Traldi, P.; Stone, J. A.; Jacobs, W. B. *Can. J. Chem.* **1994**, *72*, 966–976.
- (47) Traldi, P.; Catinella, S.; March, R. E.; Creaser, C. S. In *Practical Aspects of Ion Trap Mass Spectrometry*; March, R. E., Todd, J. F. J., Eds.; CRC Press: Boca Raton, 1995; Vol. I, p 299.
- (48) Vachet, R. W.; Glish, G. L. *Anal. Chem.* **1998**, *70*, 340–346.
- (49) Vachet, R. W.; Glish, G. L. *J. Am. Soc. Mass Spectrom.* **1998**, *9*, 175–177.
- (50) Asano, K. G.; Butcher, D. J.; Goeringer, D. E.; McLuckey, S. A. *J. Mass Spectrom.* **1999**, *34*, 691–698.
- (51) Knight, R. D. *Int. J. Mass Spectrom. Ion Phys.* **1983**, *51*, 127–131.
- (52) Wyttenbach, T.; von Helden, G.; Bowers, M. T. *J. Am. Chem. Soc.* **1996**, *118*, 8355–8354.
- (53) Counterman, A. E.; Valentine, S. J.; Srebalus, C. A.; Henderson, S. C.; Hoaglund, C. S.; Clemmer, D. E. *J. Am. Soc. Mass Spectrom.* **1998**, *9*, 743–759.
- (54) Schnier, P. D.; Price, W. D.; Strittmatter, E. F.; Williams, E. R. *J. Am. Soc. Mass Spectrom.* **1997**, *8*, 771–780.
- (55) Freitas, M. A.; Hendrickson, C. L.; Emmett, M. R.; Marshall, A. G. *J. Am. Soc. Mass Spectrom.* **1998**, *9*, 1012–1019.
- (56) Freitas, M. A.; Marshall, A. G. *Int. J. Mass Spectrom.* **1999**, *182/183*, 221–231.
- (57) Schaaff, T. G.; Stephenson, J. L., Jr.; McLuckey, S. A. *J. Am. Chem. Soc.*, in press.
- (58) Thorne, G. C.; Ballard, K. D.; Gaskell, S. J. *J. Am. Soc. Mass Spectrom.* **1990**, *1*, 249–257.
- (59) McLuckey, S. A.; Van Berkel, G. J.; Glish, G. L. *J. Am. Chem. Soc.* **1990**, *112*, 5668–5670.
- (60) Ikonou, M. G.; Kebarle, P. *Int. J. Mass Spectrom. Ion Processes* **1992**, *117*, 283–298.
- (61) Gross, D. S.; Williams, E. R. *J. Am. Chem. Soc.* **1995**, *117*, 883–890.
- (62) Zhang, X.; Cassady, C. J. *J. Am. Soc. Mass Spectrom.* **1996**, *7*, 1211–1218.
- (63) Williams, E. R. *J. Mass Spectrom.* **1996**, *31*, 831–842.